Energy conservation by oxidation of formate to carbon dioxide and hydrogen via a sodium ion current in a hyperthermophilic archaeon

Jae Kyu Lim[a,b], Florian Mayer[c], Sung Gyun Kang[a,b,1], and Volker Müller[c,1]

[a]Korea Institute of Ocean Science and Technology, 787 Haeanro, Ansan 426-744, South Korea; [b]Department of Marine Biotechnology, University of Science and Technology, Daejeon 350-333, South Korea; and [c]Department of Molecular Microbiology and Bioenergetics, Institute of Molecular Biosciences, Johann Wolfgang Goethe University Frankfurt/Main, 60438 Frankfurt, Germany

Edited by Caroline S. Harwood, University of Washington, Seattle, WA, and approved June 25, 2014 (received for review April 17, 2014)

Thermococcus onnurineus **NA1 is known to grow by the anaerobic oxidation of formate to CO_2 and H_2, a reaction that operates near thermodynamic equilibrium. Here we demonstrate that this reaction is coupled to ATP synthesis by a transmembrane ion current. Formate oxidation leads to H^+ translocation across the cytoplasmic membrane that then drives Na^+ translocation. The ion-translocating electron transfer system is rather simple, consisting of only a formate dehydrogenase module, a membrane-bound hydrogenase module, and a multisubunit Na^+/H^+ antiporter module. The electrochemical Na^+ gradient established then drives ATP synthesis. These data give a mechanistic explanation for chemiosmotic energy conservation coupled to formate oxidation to CO_2 and H_2. Because it is discussed that the membrane-bound hydrogenase with the Na^+/H^+ antiporter module are ancestors of complex I of mitochondrial and bacterial electron transport these data also shed light on the evolution of ion transport in complex I-like electron transport chains.**

ATP synthase | proton potential | sodium ion potential | bioenergetics

Formate is a common end product of bacterial fermentation and is liberated into the environment. It does not accumulate but is oxidized under oxic as well as anoxic conditions. Oxidation of formate to CO_2 and H_2 under anoxic conditions according to

$$HCOO^- + H_2O \rightarrow HCO_3^- + H_2 \quad \Delta G^0 = +1.3 \text{ kJ/mol} \qquad [1]$$

is an endergonic process under standard conditions at 25 °C. Nevertheless, some anaerobic microbes can grow by this reaction. In anaerobic syntrophic formate oxidation the reaction is made thermodynamically possible by removal of the end product H_2 by a methanogenic or sulfate-reducing partner (1–4). For pure cultures, growth at the expense of Eq. **1** was considered impossible owing to the thermodynamic constraints (2, 3). However, recently we reported that several hyperthermophilic archaea belonging to the family *Thermococcales*, including *Thermococcus onnurineus* NA1, are able to grow by oxidation of formate to molecular hydrogen (5, 6). At 80 °C, the optimum growth temperature for these hyperthermophiles, the reaction becomes slightly exergonic ($\Delta G^0 = -2.6$ kJ/mol), according to the Van't Hoff equation (7). Measurements of pool sizes of products and educts of the reaction catalyzed by whole cells at 80 °C revealed that the ΔG was more negative and growth occurred within a range of concentrations of products and educts that equals −20 to −8 kJ/mol (5), indicating that the reaction is potentially able to drive formation of an electrochemical ion gradient across the membrane.

Molecular and genetic analyses revealed that the hydrogenase genes in the *fdh2-mfh2-mnh2* gene cluster are essential for growth coupled to formate oxidization and hydrogen production (5, 8). Based on these findings a model was developed in which the formate dehydrogenase (Fdh2) module oxidizes formate; the hydrogenase (Mfh2) module transfers electrons to protons, thereby generating a proton gradient across the membrane that is then used by the Mnh2 module to produce a secondary sodium ion gradient that then drives ATP synthesis, catalyzed by a Na^+-ATP synthase (2, 5).

In this work, we will show that formate oxidation is indeed coupled to H^+ and Na^+ efflux from the cells and that the Na^+ gradient drives the synthesis of ATP. Mutant analyses are consistent with a role of the Na^+/H^+ antiporter (Mnh) module in Na^+ export. This is the first example to our knowledge of a chemiosmotic mechanism of ATP synthesis with Na^+ as coupling ion coupled to formate oxidation to carbon dioxide and hydrogen.

Results

Sodium Ions Stimulate Hydrogen Production and ATP Synthesis Driven by Formate Oxidation. To address a potential involvement of Na^+ in energy conservation in *T. onnurineus* NA1, the effect of Na^+ on H_2 production from formate and ATP synthesis was monitored. After addition of sodium formate to cell suspensions of *T. onnurineus* NA1, H_2 was produced and ATP was synthesized (Fig. 1). In contrast, ATP production was not observed after addition of potassium formate but was restored by addition of NaCl to the assay. The Na^+ concentration in the buffer without added Na^+ was less than 100 μM, as determined by inductively coupled plasma atomic emission spectroscopy. These data clearly demonstrate a role of Na^+ in ATP synthesis and/or its coupling to formate oxidation. Hydrogen production was also stimulated by Na^+ to a great extent; maximal hydrogen production was observed at 100 mM NaCl (Fig. 1).

Next, we tested the energetics of ATP synthesis. The protonophore 3,3′,4′,5-tetrachlorosalicylanilide (TCS) completely abolished ATP synthesis, clearly showing an involvement of a transmembrane proton gradient in ATP synthesis (Fig. S1).

Significance

We report here that oxidation of formate to CO_2 and H_2 that operates close to thermodynamic equilibrium is coupled to vectorial H^+ and Na^+ transport across the cytoplasmic membrane of the hyperthermophilic archaeon *Thermococcus onnurineus* NA1. The ion gradient established then drives ATP synthesis via a Na^+-ATP synthase. The energy-converting enzyme complex involves a formate dehydrogenase, a membrane-bound hydrogenase with similarity to complex I of the aerobic electron transport chain and a multisubunit Na^+/H^+ antiporter.

Author contributions: J.K.L., S.G.K., and V.M. designed research; J.K.L. and F.M. performed research; F.M. contributed new reagents/analytic tools; J.K.L., S.G.K., and V.M. analyzed data; and J.K.L., F.M., S.G.K., and V.M. wrote the paper.

The authors declare no conflict of interest.

This article is a PNAS Direct Submission.

[1]To whom correspondence may be addressed. Email: sgkang@kiost.ac or vmueller@bio.uni-frankfurt.de.

This article contains supporting information online at www.pnas.org/lookup/suppl/doi:10.1073/pnas.1407056111/-/DCSupplemental.

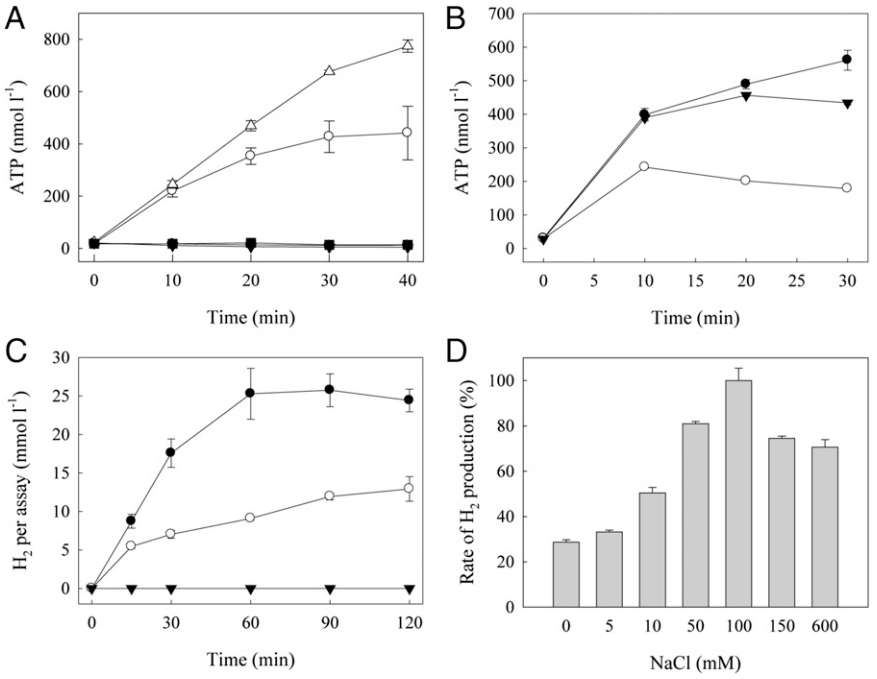

Fig. 1. Na^+- dependent ATP synthesis in resting cell suspensions. (*A*) Cells were suspended in sodium-free buffer to OD_{600} 0.5. The cellular ATP content was determined in the absence of formate (●) or presence of 150 mM sodium formate (○), 150 mM potassium formate (▼), 150 mM NaCl with 150 mM potassium formate (△), and 150 mM NaCl with 150 mM KCl (■). (*B*) Effect of Na^+/H^+ antiporter inhibitor, EIPA, on ATP synthesis. ATP synthesis was assayed by cell suspension of wild-type NA1 in the absence (●) or presence (○) of 60 mM ethyl isopropyl amiloride (EIPA), an inhibitor of Na^+/H^+ antiporter. A control received the solvent DMSO only (▼). The reaction mixture contained 150 mM potassium formate and 10 mM NaCl. (*C*) H_2 concentration in a cell suspension of wild-type NA1 incubated with different formate salts: 150 mM sodium formate (●), 150 mM potassium formate (○), and absent of formate (▼). (*D*) H_2 content in the assay at different concentrations of NaCl (measured after 60 min of incubation; for 100% value, see *C*).

The Na^+/H^+ antiport inhibitor ethyl isopropyl amiloride (EIPA) (9) had little effect on the electron input and output modules but reduced ATP synthesis by 60%, indicating that the conversion of a proton gradient to a sodium ion gradient is involved in ATP synthesis. Finally, the ATP synthase inhibitor N,N′-dicyclohexylcarbodiimide (DCCD) had no effect on hydrogen production or Fdh activity but completely inhibited ATP synthesis (Fig. S1). The inhibitor profiling is consistent with the following sequence of events: Formate oxidation is coupled to the generation of a proton gradient that is then converted to a sodium ion gradient that then drives ATP synthesis via the A_1A_O ATP synthase.

***mnh2* Mutants Are Impaired in Growth on and Hydrogen Production from Formate.** To determine the role of the Mnh2 module in formate respiration, mutants were constructed (Table 1). The multisubunit Na^+/H^+ antiporter is encoded by seven genes, and the mutants generated had all genes (Δ*mnh2ABCDEFG*) or *mnhA-D* or *mnhG* deleted. Growth of any Δ*mnh2* mutant in rich medium, ASW-YT, closely resembled growth of the wild-type strain (Fig. S2), but formate-dependent growth was abolished in every mutant (Fig. 2). At the same time, cell suspensions of the mutants no longer produced hydrogen from formate, nor did they synthesize ATP after addition of formate (Fig. 2). The same phenotype was observed for a Δ*fhh2* and Δ*mfh2* mutant, respectively. These data indicate a strict coupling of Mnh2 activity to Mfh2 and Fdh activity and revealed that Mnh2 is essential for ATP synthesis.

Formate Oxidation Is Coupled to Proton Efflux in the Absence of Na^+. Next, we tested whether electron transfer from formate to protons is coupled to proton translocation across the cytoplasmic membrane. Therefore, inverted vesicles were prepared as described in the experimental procedures. They contained formate dehydrogenase (Fdh2), hydrogenase (Mfh2), and the Na^+/H^+ antiporter module (Mnh2), as demonstrated by Western blot analysis and the presence of the enzymatic activities (Fig. S3). A possible proton efflux coupled to formate oxidation was measured using the pH-sensitive dye 9-amino-6-chloro-2-methoxyacridine (ACMA), whose fluorescence is quenched by a decrease in pH. As shown in Fig. 3, the addition of calcium formate to inverted vesicles incubated in the absence of Na^+ led to a gradual decrease in the fluorescence intensity of ACMA, indicative of active proton transport. Addition of NH_4Cl in the steady state of quenching led to an immediate dequenching, which is evidence that indeed a ΔpH across the membrane had been built up. The ΔpH was also dissipated by addition of NaCl, but not KCl, indicating the presence of a Na^+/H^+ antiporter activity in the cytoplasmic membrane. Addition of potassium formate also drove proton influx into the inverted vesicles. Consistent with the experiment using resting cell suspension, the proton gradient was dissipated by the addition of the protonophore TCS (Fig. 3*B*). Moreover, copper ions not only completely inhibited proton gradient formation but also ATP synthesis (Fig. 3*C* and Fig. S1*C*).

Formate Oxidation Is Coupled to Na^+ Efflux. The fact that formate-driven proton transport was only observed in the absence of Na^+ and that the established proton gradient was dissipated after addition of Na^+ led us to speculate that formate-driven hydrogen production is coupled to Na^+ export. This was tested using inverted vesicles incubated in the presence of $^{22}Na^+$. Upon addition of formate to these vesicles, Na^+ was translocated into their lumen with an initial rate of 11.6 nmol·min^{-1}·mg protein^{-1} up to a final accumulation factor of 6.8 (Fig. 4). Sodium transport was dependent on formate and completely impaired by the sodium ionophore N,N,N,N′-tetra-cyclo-hexyl-1,2-phenylenedioxydiacetamide (ETH2120). The protonophore TCS also inhibited $^{22}Na^+$ transport, but to a smaller extent (39% of the rate). $^{22}Na^+$ transport was slightly inhibited by the ATPase

Table 1. *T. onnurineus* NA1 wild-type and mutant strains used in this study

Strain	Genotype*	Source
NA1	Wild-type Sim^s	53
Δ*fdh2*	NA1 Δ*fdh2::hmg* Sim^r	This study
Δ*mfh2*	NA1 Δ*mfh2::hmg* Sim^r	5
Δ*mnh2-1*	NA1 Δ*mnh2ABCDEFG::hmg* Sim^r	This study
Δ*mnh2-2*	NA1 Δ*mnh2ABCD::hmg* Sim^r	This study
Δ*mnh2-3*	NA1 Δ*mnh2G::hmg* Sim^r	This study

*Sim^s, simvastatin-sensitive; Sim^r, simvastatin-resistant.

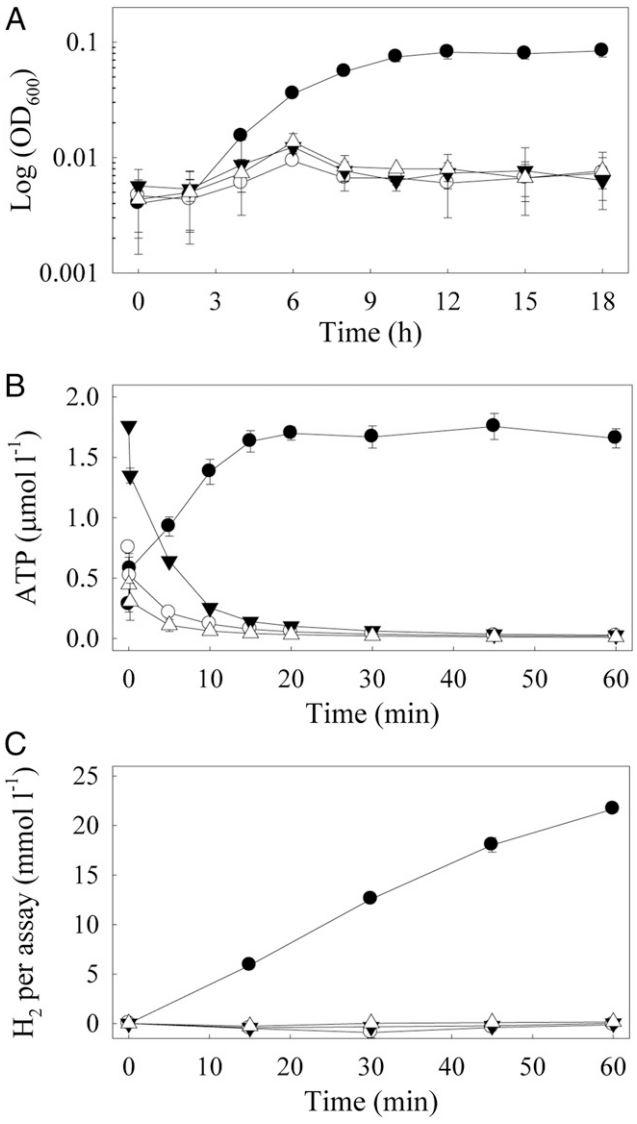

Fig. 2. Changes in physiology of mutant strains: (*A*) cell growth, (*B*) ATP synthesis, and (*C*) hydrogen content. MM1 medium with 3 g·L^{-1} tryptone was used as a culture medium for preparation of cell suspension. Symbols indicate *T. onnurinues* NA1 wild type (●), Δ*fdh2* (○), Δ*mfh2* (▼), and Δ*mnh2-1* (△). The cellular ATP levels decrease during harvest but the rate of decrease is variable in different cell suspensions, leading to different "zero" values.

inhibitor DCCD, whereas the ATPase inhibitor diethylstilbestrol (DES) had only a negligible effect (Fig. 4*B*). These data clearly demonstrate sodium ion transport coupled to formate oxidation in *T. onnurineus* NA1.

The ATP Synthase Translocates Na^+. The experiments described so far are consistent with the hypothesis that formate oxidation leads to a secondary Na^+ gradient that then drives ATP synthesis. If this is true, the ATP synthase should use Na^+, not H^+, as coupling ion. To address this question ATP-dependent ion translocation was monitored. Addition of ATP to inverted vesicles did not lead to proton transport (as determined by ACMA quenching). However, after addition of ATP to inverted vesicles $^{22}Na^+$ was translocated into the lumen at a rate of 15.5 nmol·min^{-1}·mg^{-1} up to a final accumulation factor of 10.5 (Fig. 5). Na^+ transport was ATP-dependent and completely inhibited by the Na^+ ionophore ETH2120. Na^+ transport was electrogenic, as evident from the stimulation by the protonophore TCS. ATP-dependent Na^+ transport was inhibited by the ATPase inhibitors DCCD and DES (Fig. 5*B*), indicating that ATP-driven Na^+ transport is catalyzed by the A_1A_O ATP synthase.

Discussion

Chemiosmotic coupling of exergonic metabolic reactions to ATP synthesis is the most widely distributed and also most ancient mechanism of energy conservation in living cells (2, 10, 11). It may have derived as a means for coupling in organisms that live on "low-energy" substrates that do not even allow for the synthesis of 1 mol of an ATP per mole of substrate converted. The low energy content of these substrates excludes a direct coupling

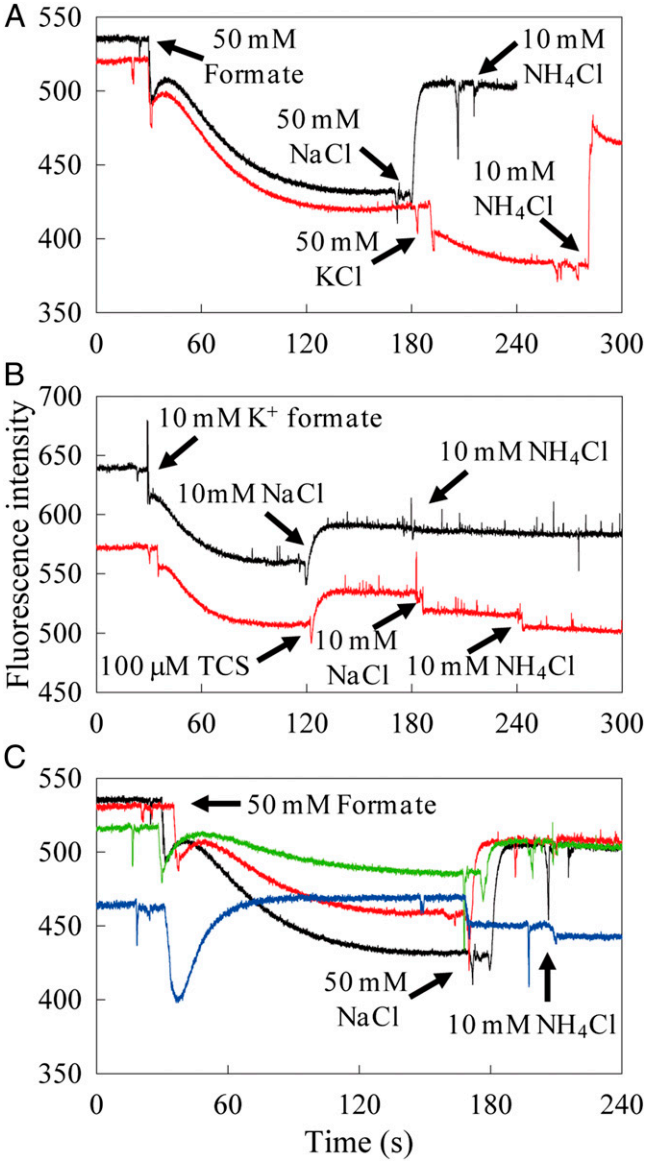

Fig. 3. Formate oxidation leads to a ΔpH in inverted membrane vesicles. ΔpH was measured using ACMA. (*A*) Respiration was initiated by addition of 50 mM formic acid the pH adjusted to 6.5 by $Ca(OH)_2$. Fifty millimolar NaCl (black line) and KCl (red line) were added to the mixture at the times indicated by black arrows. (*B*) Experimental conditions as in *A*. Respiration was initiated by addition of 10 mM potassium formate; 100 μM TCS was added to dissipate the H^+ gradient (red line). (*C*) The reaction mixture was preincubated in the absence (black line; positive control) or presence of 20 (red line), 50 (green line), or 100 μM (blue line) $CuCl_2$. The experimental procedures were as in *A*.

MICROBIOLOGY

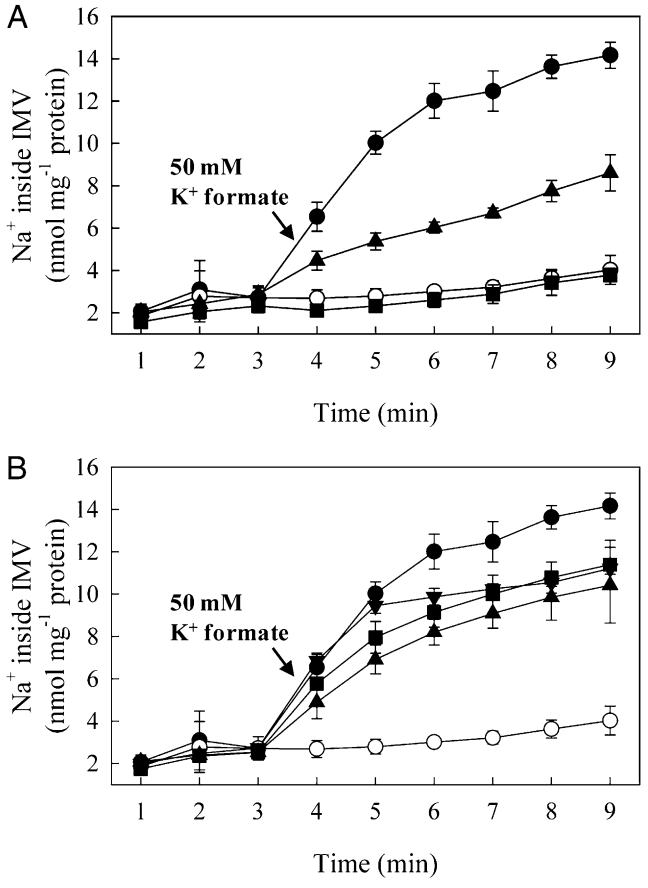

Fig. 4. Na^+ transport coupled to formate oxidation. (*A*) Ionophore effect: 50 mM potassium formate (●), absence of formate (○), 50 mM potassium formate with 100 μM TCS (▲), and 50 mM potassium formate with 50 μM ETH2120 (■). (*B*) Inhibitor effect: 50 mM potassium formate (●), absence of formate (○), 1 mM $CuCl_2$ (■), 10 μM DCCD (▲), and 100 μM DES (▼).

of an exergonic metabolic reaction to ATP synthesis by a direct coupling mechanism that would require ~60 kJ/mol ATP under cellular conditions. Instead, the exergonic metabolic reaction may be coupled first to an export of an ion across the cytoplasmic membrane and the established transmembrane electrochemical sodium ion gradient then drives ATP synthesis. If we consider an ion/ATP stoichiometry of 4, the metabolic reaction has to proceed four times to translocate the amount of ions necessary to make one ATP. In this scenario, the minimal biological energy quantum is the amount of energy required to translocate an ion across the cytoplasmic membrane. Methanogenic archaea have a methyltransferase that catalyze methyl transfer from methyltetrahydromethanopterin to coenzyme M. The $\Delta G^{0'}$ of the reaction is only −30 kJ/mol, enough to translocate approximately two Na^+ across the cytoplasmic membrane (12). Other examples are the Na^+-translocating ferredoxin: NAD oxidoreductase of bacteria (13, 14) and the Ech hydrogenase of bacteria and archaea (15, 16). The latter enzyme catalyzes electron transfer from reduced ferredoxin to protons ($\Delta G^{0'}$ = −19.3 kJ/mol), coupled to proton translocation across the membrane. A similar reaction is catalyzed by the membrane-bound hydrogenase of *Pyrococcus furiosus* that also uses electron transfer from reduced ferredoxin to protons to establish a transmembrane ion gradient (17). Here we describe a reaction that operates at even smaller free-energy changes. Obviously, electron flow from formate to protons allows for the generation of a transmembrane ion gradient. The experimentally determined values of −8 to −20 kJ for the free-energy change associated with formate oxidation to CO_2 and H_2 (8) are sufficient to translocate 0.5–1.2 Na^+ out of the cell at a transmembrane electrochemical Na^+ potential of −180 mV. If we assume a Na^+/ATP stoichiometry of 4, this would allow for only 0.125–0.3 mol ATP per mole of formate.

How can a net translocation of less than one ion per substrate be achieved? First, the magnitudes of the transmembrane electrochemical ion gradients are not known in hyperthermophilic archaea. If it would be as low as −90 mV [the minimal amount of energy required for ATP synthesis in a bacterial enzyme (18)], a ΔG of −8 kJ/mol would be enough to drive the export of an ion. At electrochemical potentials around −180 mV (which is roughly the value in the few bacteria and archaea analyzed), values lower than 1 are possible using two chemiosmotic enzymes operating together with different ion stoichiometries. Whether the Fdh2–MfH2 module acts like a classical redox loop or more like a proton pump remains to be established, but the apparent lack of quinone biosynthesis genes in the genome and the similarity of the Mfh2 module to complex I of the respiratory chain is not consistent with a redox-like, but rather a pump-like, mechanism for ion translocation. Anyway, chemiosmotic enzymes may operate at different stoichiometries. If, for example, one proton is "extruded" in the course of the Fdh2/Mfh2 catalyzed reaction, the Na^+/H^+ antiporter Mnh must have a Na^+/H^+ stoichiometry <1 to get a Na^+/HCOOH stoichiometry below 1. This would require that the H^+ and Na^+ potentials operate at different magnitudes. Chemiosmotic enzymes may in addition use flexible stochiometries and may thus have evolved as a solution to live on low ΔG energy sources.

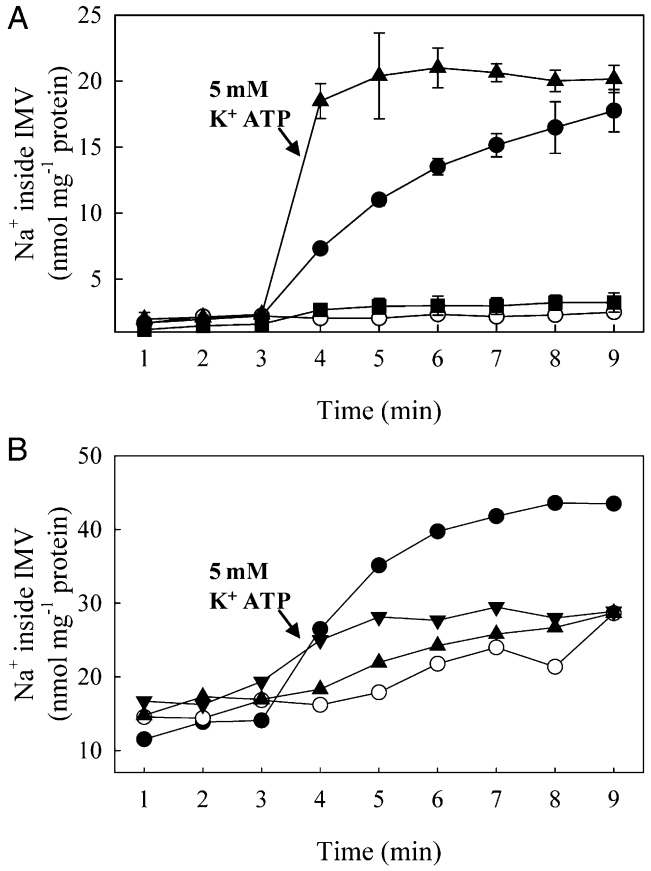

Fig. 5. Na^+ transport coupled to ATP hydrolysis. (*A*) Ionophore effect: 5 mM potassium ATP (●), absence of ATP (○), 5 mM potassium ATP with 100 μM TCS (▲), and 5 mM potassium ATP with 50 μM ETH2120 (■). (*B*) Inhibitor effect: 5 mM potassium ATP (●), absence of ATP (○), 500 μM DCCD (▲), and 100 μM DES (▼).

The data presented here are in accordance with an electron transfer from the formate dehydrogenase module to the hydrogenase module and its coupling to H^+ export. The proton is then exchanged to Na^+ by the Na^+/H^+ antiporter module and the secondary Na^+ gradient then drives ATP synthesis. In a recent study it was reported that expression of the *fdh2-mfh2-mnh2* gene cluster of *T. onnurineus* in *P. furiosus* did not result in growth of *P. furiosus* on formate, and this was interpreted to exclude energy conservation coupled to this reaction (19). However, it has to be kept in mind that growth of the transformant not only requires energy conservation but also biosynthesis of cell mass from formate or CO_2.

Respiratory chains have different modules that transfer electrons from a donor to an acceptor. Complex I of the aerobic respiratory chain in mitochondria and some bacteria is the entry port of electrons derived from NADH. It is an L-shaped molecule that in bacteria consists of 14 subunits. The NADH binding site is at the distal end of the hydrophilic domain and electrons travel down to the membrane by a chain of iron–sulfur centers to quinones. The quinone-binding site is at the proximal end of the hydrophilic domain. Electron transport is coupled to conformational changes in the membrane domain that leads to ion translocation. The membrane domain has a row of four modules with similarities to Na^+/H^+ antiporter that are assumed to catalyze proton transport. Whether or not sodium ions are transported as well is still a matter of debate (20–28). Complex I is an example of an energy-converting enzyme with a modular structure composed of an electron donor/transfer module (encoded by *nuoE*, *F*, and *G*), connecting module (encoded by *nuoC*, *D*, *B*, and *I*), and intrinsic membrane module (encoded by *nuoH*, *N*, *A*, *M*, *K*, *L*, and *J*). Interestingly, the electron donor module is very similar to group 4 hydrogenases (15, 27, 29–35).

Group 4 hydrogenases are widely distributed among bacteria and archaea (33), including Hyc and Hyf (hydrogenase 3 and 4, respectively) from *Escherichia coli* (36), Coo (CO-induced hydrogenase) from *Rhodospirillum rubrum* (37), Ech (energy-converting hydrogenase) from *Methanosarcina barkeri* (38), Mbh (membrane-bound hydrogenase) from *P. furiosus* (39, 40), and the membrane-bound hydrogenase module Mfh2 from *T. onnurineus* NA1. They all are key enzymes in hydrogen production and have been hypothesized to be energy-converting, based on similarity to complex I. This has been experimentally shown for Mbh and Ech (15, 17, 35, 39) using inverted membrane vesicle preparations. The coupling ion has not been addressed experimentally but was hypothesized to be proton. Mfh2 of *T. onnurineus* NA1 is suggested to be coupled to H^+ translocation.

A multisubunit Na^+/H^+ antiporter module is also found in complex I (41, 42). However, there is no report to unveil the physiological role of multisubunit monovalent cation/proton antiporter participating in mediating the electron relay of the respiratory chain to date. The multisubunit monovalent cation/proton antiporter (Mrp homologs) have been mainly studied in bacteria and attributed to physiological functions such as pH homeostasis and Na^+ resistance (43, 44), cell sporulation (45), symbiotic nitrogen fixation (46), arsenite resistance (47), and bile salt resistance (48–50), whereas in archaea alternative Mrp-like gene clusters were found, so-called group 3 Mrp, and some of them are found in the membrane bound hydrogenase Mbh (44). The data presented here are consistent with the hypothesis that the Mnh2 module converts the H^+ gradient established by the Mfh2 module to a secondary Na^+ gradient. Although it is still debated whether complex I is an (outwardly directed) Na^+ pump, evidence was presented for Na^+ influx through complex I in *Rhodothermus marinus* (28). Na^+ influx is suggested to drive H^+ export and is dependent on menaquinone reduction (51). Modern complex I enzymes may have lost the Na^+/H^+ antiport activity because they operate with high ΔG sources such as the NADH/quinone pair.

The electrochemical Na^+ gradient drives ATP synthesis via a Na^+-translocating ATP synthase. The latter would not be unusual and, in fact, has been described for some archaea (52). *T. onnurineus* NA1 apparently uses a Na^+ current across its membrane for ATP synthesis. The use of Na^+ as coupling ion is an advantage for microbes living at the thermodynamic limit (2), but sodium ion transport was apparently lost in "modern" complex I enzymes, although it may be retained in some marine species (28).

Materials and Methods

Strain and Cell Culture Conditions. *T. onnurineus* NA1 (KCTC 10859) was isolated from a deep-sea hydrothermal vent area in the Papua New Guinea–Australia–Canada–Manus field (53). This strain was routinely cultured in modified medium 1 (MM1) (5, 54) and ASW-YT medium (55) containing 4 $g{\cdot}L^{-1}$ of elemental sulfur used as a rich medium. All procedures for cultivation of *T. onnurineus* NA1 were conducted as previously described (5, 8, 56). Mutants were grown in MM1 medium containing 3 $g{\cdot}L^{-1}$ tryptone. For maintaining anaerobic conditions, all procedures were carried out in an anaerobic chamber (Coy Laboratory Products).

The pH-stat fed-batch culture of *T. onnurineus* NA1 was anaerobically carried out in a 7-L fermentor with a working volume of 4 L using the MM1 medium with 4 $g{\cdot}L^{-1}$ of yeast extract and 400 mM sodium formate. The culture temperature and agitation speed were 80 °C and 300 rpm, respectively, and the pH was controlled at 6.1–6.2 by automatic titration with 4 M formic acid in 3.5% NaCl. The medium of the fermentor was flushed with argon gas for 10 min before inoculation.

Preparation of Cell Suspensions. To prepare cell suspensions, *T. onnurineus* NA1 was anaerobically cultured in a 7-L fermentor with a working volume of 4 L as described above. At the end of the culture, the cells were harvested by centrifugation at 5,523 × *g* for 30 min at 20 °C. Cell suspensions were prepared by washing the harvested cells with an anaerobic and sodium free modified Buffer-A (20 mM imidazole/HCl, 30 mM $MgCl_2$, 1 M KCl, and 2 mM DTT, pH 6.5) and resuspending them in the same buffer at cell densities of OD_{600} = 0.5.

Preparation of Inverted Membrane Vesicles. Inverted membrane vesicles were prepared under strictly anaerobic condition at 25 °C. Typically 2–4 g (wet weight) of fed-batch cultured *T. onnurineus* NA1 cell pellets were harvested and washed with a suspension buffer [10 mM Tris·HCl, 140 mM choline chloride, 10% (vol/vol) glycerol, protease inhibitor mixture tablets (Roche Diagnostics), and 2 mM DTT, pH 7.5]. For $^{22}Na^+$ translocation experiments the membrane vesicles were prepared by passing through a French pressure cell (Aminco) at 8,000 psi one time. Inverted membrane vesicles for all other experiments were prepared via disruption by sonication. To remove cell debris, the cell lysate was centrifuged at 10,000 × *g* for 15 min at 25 °C and the lysate was transferred to a new tube. Membranes were pelleted by ultracentrifugation at 120,000 × *g* for 1.5 h at 25 °C. The pellet was washed twice and resuspended with a suspension buffer to a concentration of ~20 $mg{\cdot}mL^{-1}$ of protein. The presence of vesicles was confirmed by transmission electron microscope.

Enzyme Assays. For H_2 production and ATP synthesis, cell suspensions in the modified Buffer-A at a final cell density of OD_{600} = 0.5 were used (5, 8). Cell suspensions were incubated at 60 °C. To determine H_2 production a rubber-sealed glass vial was used. The reaction was initiated by the addition of 150 mM potassium formate. At various time intervals, gas samples were taken and analyzed in a YL6100 GC gas chromatograph (YL Instrument) for H_2 and liquid samples to determine the ATP content. Therefore, 50-μL aliquots were added to 450 μL of DMSO for 1 min to stop the reaction before the measurement of ATP using an Enliten luciferin/luciferase kit (Promega).

Measurement of ΔpH. Measurements of ΔpH were conducted in a 2-mL volume of AA-buffer containing 5 μM ACMA and 0.5 mg of inverted membrane vesicles in a serum-stoppered crystal cuvette. The reaction mixture was preincubated at 60 °C for 10 min and then respiration was initiated by the addition of potassium formate or formic acid [pH was adjusted to pH 6.5 by $Ca(OH)_2$] to a final concentration of 50 mM. Fluorescence was detected using a RF-5301PC spectrofluorophotometer (Shimadzu) with excitation at 410 nm (3-mm slit) and emission at 480 nm (3-mm slit), maintaining the reaction temperature at 60 °C. Addition of 10 mM ammonium chloride was used to dissipate the remaining ΔpH to bring the fluorescence back to baseline.

Measurement of Na^+ Translocation. Na^+ translocation measurements coupled to ATP hydrolysis were performed in ATP hydrolysis buffer [100 mM Tris (pH 7), 10

mM $MgCl_2$, and 60 mM $NaHSO_3$] and Na^+ translocation measurements coupled to formate oxidation were performed in AA-buffer. The protein concentration and sodium concentration as well as ionophore and inhibitor concentrations used are as indicated. The ionophores ETH2120 and TCS as well as the ATPase inhibitors DCCD and DES were added from DMSO stock solutions and controls received the solvent only. In a 3.5-mL glass vial, the inverted membrane vesicles, the buffer, supplements, and $^{22}NaCl$ (carrier-free, final activity 0.5 μCi/mL) were mixed and incubated at 60 °C for 30 min to ensure equilibration of $^{22}Na^+$. After that the reaction was started with the addition of 5 mM potassium ATP or 50 mM potassium formate. Eighty-microliter samples were taken and passed over a column (0.5 × 3.2 cm) of Dowex 50-WX8 (100–200 mesh) according to Heise et al. (57). By washing the column with 1 mL of 420 mM sucrose, the inverted membrane vesicles were collected. The radioactivity of the elution fractions was determined using liquid scintillation counting.

ACKNOWLEDGMENTS. This work was supported by Korea Institute of Ocean Science and Technology in-house program Grants PE99212 and PE99263 and the Development of Biohydrogen Production Technology Using the Hyperthermophilic Archaea program of the Ministry of Oceans and Fisheries (to S.G.K.) as well as by the Deutsche Forschungsgemeinschaft through Grants SFB 807 and MU801/15-1 (to V.M.).

1. Jackson BE, McInerney MJ (2002) Anaerobic microbial metabolism can proceed close to thermodynamic limits. *Nature* 415(6870):454–456.
2. Mayer F, Müller V (2014) Adaptations of anaerobic archaea to life under extreme energy limitation. *FEMS Microbiol Rev* 38(3):449–472.
3. Schink B (1997) Energetics of syntrophic cooperation in methanogenic degradation. *Microbiol Mol Biol Rev* 61(2):262–280.
4. Stams AJ, Plugge CM (2009) Electron transfer in syntrophic communities of anaerobic bacteria and archaea. *Nat Rev Microbiol* 7(8):568–577.
5. Kim YJ, et al. (2010) Formate-driven growth coupled with H_2 production. *Nature* 467(7313):352–355.
6. Lee HS, et al. (2008) The complete genome sequence of *Thermococcus onnurineus* NA1 reveals a mixed heterotrophic and carboxydotrophic metabolism. *J Bacteriol* 190(22):7491–7499.
7. Conrad R, Wetter B (1990) Influence of temperature on energetics of hydrogen metabolism in homoacetogenic, methanogenic, and other anaerobic bacteria. *Arch Microbiol* 155:94–98.
8. Lim JK, et al. (2012) Thermodynamics of formate-oxidizing metabolism and implications for H_2 production. *Appl Environ Microbiol* 78(20):7393–7397.
9. Becher B, Müller V (1994) $\Delta\mu_{Na^+}$ drives the synthesis of ATP via an $\Delta\mu_{Na^+}$-translocating F_1F_0-ATP synthase in membrane vesicles of the archaeon *Methanosarcina mazei* Gö1. *J Bacteriol* 176(9):2543–2550.
10. Mitchell P (1972) Chemiosmotic coupling in energy transduction: A logical development of biochemical knowledge. *J Bioenerg* 3(1):5–24.
11. Martin WF (2012) Hydrogen, metals, bifurcating electrons, and proton gradients: The early evolution of biological energy conservation. *FEBS Lett* 586(5):485–493.
12. Gottschalk G, Thauer RK (2001) The Na^+-translocating methyltransferase complex from methanogenic archaea. *Biochim Biophys Acta* 1505(1):28–36.
13. Biegel E, Müller V (2010) Bacterial Na^+-translocating ferredoxin:NAD^+ oxidoreductase. *Proc Natl Acad Sci USA* 107(42):18138–18142.
14. Biegel E, Schmidt S, González JM, Müller V (2011) Biochemistry, evolution and physiological function of the Rnf complex, a novel ion-motive electron transport complex in prokaryotes. *Cell Mol Life Sci* 68(4):613–634.
15. Hedderich R, Forzi L (2005) Energy-converting [NiFe] hydrogenases: More than just H_2 activation. *J Mol Microbiol Biotechnol* 10(2-4):92–104.
16. Welte C, Krätzer C, Deppenmeier U (2010) Involvement of Ech hydrogenase in energy conservation of *Methanosarcina mazei*. *FEBS J* 277(16):3396–3403.
17. Sapra R, Bagramyan K, Adams MW (2003) A simple energy-conserving system: Proton reduction coupled to proton translocation. *Proc Natl Acad Sci USA* 100(13):7545–7550.
18. Kaim G, Dimroth P (1998) Voltage-generated torque drives the motor of the ATP synthase. *EMBO J* 17(20):5887–5895.
19. Lipscomb GL, et al. (2014) Engineering hydrogen gas production from formate in a hyperthermophile by heterologous production of an 18-subunit membrane-bound complex. *J Biol Chem* 289(5):2873–2879.
20. Weiss H, Friedrich T, Hofhaus G, Preis D (1991) The respiratory-chain NADH dehydrogenase (complex I) of mitochondria. *Eur J Biochem* 197(3):563–576.
21. Friedrich T, et al. (1993) Attempts to define distinct parts of NADH:ubiquinone oxidoreductase (complex I). *J Bioenerg Biomembr* 25(4):331–337.
22. Yamaguchi M, Hatefi Y (1993) Mitochondrial NADH:ubiquinone oxidoreductase (complex I): Proximity of the subunits of the flavoprotein and the iron-sulfur protein subcomplexes. *Biochemistry* 32(8):1935–1939.
23. Friedrich T (1998) The NADH:ubiquinone oxidoreductase (complex I) from *Escherichia coli*. *Biochim Biophys Acta* 1364(2):134–146.
24. Sazanov LA, Hinchliffe P (2006) Structure of the hydrophilic domain of respiratory complex I from *Thermus thermophilus*. *Science* 311(5766):1430–1436.
25. Lanciano P, Vergnes A, Grimaldi S, Guigliarelli B, Magalon A (2007) Biogenesis of a respiratory complex is orchestrated by a single accessory protein. *J Biol Chem* 282(24): 17468–17474.
26. Verkhovskaya ML, Belevich N, Euro L, Wikström M, Verkhovsky MI (2008) Real-time electron transfer in respiratory complex I. *Proc Natl Acad Sci USA* 105(10):3763–3767.
27. Efremov RG, Sazanov LA (2011) Structure of the membrane domain of respiratory complex I. *Nature* 476(7361):414–420.
28. Batista AP, Fernandes AS, Louro RO, Steuber J, Pereira MM (2010) Energy conservation by *Rhodothermus marinus* respiratory complex I. *Biochim Biophys Acta* 1797(4):509–515.
29. Friedrich T, Weiss H (1997) Modular evolution of the respiratory NADH:ubiquinone oxidoreductase and the origin of its modules. *J Theor Biol* 187(4):529–540.
30. Friedrich T, Scheide D (2000) The respiratory complex I of bacteria, archaea and eukarya and its module common with membrane-bound multisubunit hydrogenases. *FEBS Lett* 479(1-2):1–5.
31. Mathiesen C, Hägerhäll C (2003) The 'antiporter module' of respiratory chain complex I includes the MrpC/NuoK subunit — a revision of the modular evolution scheme. *FEBS Lett* 549(1-3):7–13.
32. Hedderich R (2004) Energy-converting [NiFe] hydrogenases from archaea and extremophiles: Ancestors of complex I. *J Bioenerg Biomembr* 36(1):65–75.
33. Vignais PM, Billoud B (2007) Occurrence, classification, and biological function of hydrogenases: An overview. *Chem Rev* 107(10):4206–4272.
34. Moparthi VK, Hägerhäll C (2011) The evolution of respiratory chain complex I from a smaller last common ancestor consisting of 11 protein subunits. *J Mol Evol* 72(5-6):484–497.
35. Marreiros BC, Batista AP, Duarte AM, Pereira MM (2013) A missing link between complex I and group 4 membrane-bound [NiFe] hydrogenases. *Biochim Biophys Acta* 1827(2):198–209.
36. Wu LF, Mandrand MA (1993) Microbial hydrogenases: Primary structure, classification, signatures and phylogeny. *FEMS Microbiol Rev* 10(3-4):243–269.
37. Fox JD, He Y, Shelver D, Roberts GP, Ludden PW (1996) Characterization of the region encoding the CO-induced hydrogenase of *Rhodospirillum rubrum*. *J Bacteriol* 178(21): 6200–6208.
38. Künkel A, Vorholt JA, Thauer RK, Hedderich R (1998) An *Escherichia coli* hydrogenase-3-type hydrogenase in methanogenic archaea. *Eur J Biochem* 252(3):467–476.
39. Sapra R, Verhagen MF, Adams MW (2000) Purification and characterization of a membrane-bound hydrogenase from the hyperthermophilic archaeon *Pyrococcus furiosus*. *J Bacteriol* 182(12):3423–3428.
40. Silva PJ, et al. (2000) Enzymes of hydrogen metabolism in *Pyrococcus furiosus*. *Eur J Biochem* 267(22):6541–6551.
41. Hunte C, Zickermann V, Brandt U (2010) Functional modules and structural basis of conformational coupling in mitochondrial complex I. *Science* 329(5990):448–451.
42. Efremov RG, Baradaran R, Sazanov LA (2010) The architecture of respiratory complex I. *Nature* 465(7297):441–445.
43. Hamamoto T, et al. (1994) Characterization of a gene responsible for the Na^+/H^+ antiporter system of alkalophilic *Bacillus* species strain C-125. *Mol Microbiol* 14(5):939–946.
44. Swartz TH, Ikewada S, Ishikawa O, Ito M, Krulwich TA (2005) The Mrp system: A giant among monovalent cation/proton antiporters? *Extremophiles* 9(5):345–354.
45. Kosono S, et al. (2005) Characterization of a multigene-encoded sodium/hydrogen antiporter (*sha*) from *Pseudomonas aeruginosa*: Its involvement in pathogenesis. *J Bacteriol* 187(15):5242–5248.
46. Putnoky P, et al. (1998) The *pha* gene cluster of *Rhizobium meliloti* involved in pH adaptation and symbiosis encodes a novel type of K^+ efflux system. *Mol Microbiol* 28(6):1091–1101.
47. Kashyap DR, Botero LM, Lehr C, Hassett DJ, McDermott TR (2006) A Na^+:H^+ antiporter and a molybdate transporter are essential for arsenite oxidation in *Agrobacterium tumefaciens*. *J Bacteriol* 188(4):1577–1584.
48. Dzioba-Winogrodzki J, et al. (2009) The *Vibrio cholerae* Mrp system: Cation/proton antiport properties and enhancement of bile salt resistance in a heterologous host. *J Mol Microbiol Biotechnol* 16(3-4):176–186.
49. Ito M, Guffanti AA, Oudega B, Krulwich TA (1999) *mrp*, a multigene, multifunctional locus in *Bacillus subtilis* with roles in resistance to cholate and to Na^+ and in pH homeostasis. *J Bacteriol* 181(8):2394–2402.
50. Ito M, Guffanti AA, Wang W, Krulwich TA (2000) Effects of nonpolar mutations in each of the seven *Bacillus subtilis mrp* genes suggest complex interactions among the gene products in support of Na^+ and alkali but not cholate resistance. *J Bacteriol* 182(20):5663–5670.
51. Batista AP, Marreiros BC, Pereira MM (2011) Decoupling of the catalytic and transport activities of complex I from *Rhodothermus marinus* by sodium/proton antiporter inhibitor. *ACS Chem Biol* 6(5):477–483.
52. Grüber G, Manimekalai MSS, Mayer F, Müller V (2014) ATP synthases from archaea: The beauty of a molecular motor. *Biochim Biophys Acta* 1837(6):940–952.
53. Bae SS, et al. (2006) *Thermococcus onnurineus* sp, nov., a hyperthermophilic archaeon isolated from a deep-sea hydrothermal vent area at the PACMANUS field. *J Microbiol Biotechnol* 16:1826–1831.
54. Sokolova TG, et al. (2004) The first evidence of anaerobic CO oxidation coupled with H_2 production by a hyperthermophilic archaeon isolated from a deep-sea hydrothermal vent. *Extremophiles* 8(4):317–323.
55. Sato T, Fukui T, Atomi H, Imanaka T (2003) Targeted gene disruption by homologous recombination in the hyperthermophilic archaeon *Thermococcus kodakaraensis* KOD1. *J Bacteriol* 185(1):210–220.
56. Lim JK, Kang SG, Lebedinsky AV, Lee J-H, Lee HS (2010) Identification of a novel class of membrane-bound [NiFe]-hydrogenases in *Thermococcus onnurineus* NA1 by *in silico* analysis. *Appl Environ Microbiol* 76(18):6286–6289.
57. Heise R, Müller V, Gottschalk G (1992) Presence of a sodium-translocating ATPase in membrane vesicles of the homoacetogenic bacterium *Acetobacterium woodii*. *Eur J Biochem* 206(2):553–557.